

JULY 1984

BNL-35104

Magnetic correlations in  
3d ferromagnets above  $T_c$

BNL--35104

DE04 016433

G. SHIRANE

The submitted manuscript has been authored under contract DE-AC02-76CH00016 with the Division of Basic Energy Sciences, U.S. Department of Energy. Accordingly, the U.S. Government retains a nonexclusive, royalty-free license to publish or reproduce the published form of this contribution, or allow others to do so, for U.S. Government purposes.

NOTICE

PORTIONS OF THIS REPORT ARE ILLICIBLE. It  
has been reproduced from the best available  
copy to permit the broadest possible avail-  
ability.

Workshop on Metallic Magnetism  
July 1984, Bad Honnef, Germany

CONFIDENTIAL

Magnetic Correlations in  
3d Ferromagnets above  $T_c$

by

G. SHIRANE  
Brookhaven National Laboratory  
Upton, New York 11963

A review is presented of our current neutron scattering experiments on Fe and Ni above the Curie temperature. Our experimental results show that the picture of propagating spin waves above  $T_c$ , widely accepted since 1973, is incorrect. In addition, we will demonstrate that over wide ranges of  $\omega$ ,  $q$  and temperature, both Fe and Ni, as well as  $Pd_2MnSn$ , follow a simple paramagnetic scattering function of the spin diffusion type.

DISCLAIMER

This report was prepared as an account of work sponsored by an agency of the United States Government. Neither the United States Government nor any agency thereof, nor any of their employees, makes any warranty, express or implied, or assumes any legal liability or responsibility for the accuracy, completeness, or usefulness of any information, apparatus, product, or process disclosed, or represents that its use would not infringe privately owned rights. Reference herein to any specific commercial product, process, or service by trade name, trademark, manufacturer, or otherwise does not necessarily constitute or imply its endorsement, recommendation, or favoring by the United States Government or any agency thereof. The views and opinions of authors expressed herein do not necessarily state or reflect those of the United States Government or any agency thereof.

The submitted manuscript has been authored under Contract No. De-AC02-76CH00016 with the U.S. Department of Energy. Accordingly, the U.S. Government retains a nonexclusive, royalty-free license to publish or reproduce the published form of this contribution, or allow others to do so, for U.S. Government purposes.

MASTER

DISTRIBUTION OF THIS DOCUMENT IS UNLIMITED

*J. S. ...*

## I. INTRODUCTION

We present a brief review of our current neutron scattering experiments<sup>1</sup> on 3d ferromagnets. This study started out as a re-examination of the spin waves above  $T_c$  in Fe and Ni. During the course of the experiments considerable progress has been made in the technique of polarization analysis of inelastic scattering and we have now applied this new technique for the study of other 3d ferromagnets; Fe<sub>3</sub>Pt, Pd<sub>2</sub>MnSn and MnSi. We present, in some detail, the most recent results on Fe and Ni and give an overview of the general features that have emerged from the experiments on other 3d metals, in particular Pd<sub>2</sub>MnSn.

The picture of propagating spin waves above  $T_c$  in Ni and Fe has been widely accepted since Mook, Lynn and Nicklow<sup>2</sup> published their first constant energy scan peaks in Ni in 1973. Later, additional measurements were performed on Fe by Lynn<sup>3</sup> and on Ni by Lynn and Mook.<sup>4</sup> The spin wave concept was based on the conversion of  $\Delta q/q \rightarrow \Delta E/E$  assuming that the peak positions as measured during constant E-scans determined a dispersion curve. The existence of propagating spin waves above  $T_c$  was claimed for energies exceeding 8 meV for Fe and 35 meV for Ni. These spin waves are, surprisingly, practically temperature independent up to 1.5  $T_c$ .

However, recent polarized and unpolarized neutron scattering experiments<sup>5,6</sup> performed at Brookhaven on Ni and Fe have challenged this long accepted concept. These new results demonstrate that the constant E-scans exhibit ridges at finite  $q$ , in agreement with Lynn and Mook (Fig. 1). But the spectral weight in constant Q-scans is centered around zero energy transfer: i.e., the scattering is quasielastic. This result is in agreement with recent paramagnetic scattering measurements<sup>7</sup> performed at ILL on Fe utilizing polarized neutrons with an intentionally broad resolution. Therefore, the constant E-scan peaks do not define a dispersion curve and the conversion  $\Delta q/q \rightarrow \Delta E/E$  is not

justifiable. We will describe later the conditions under which this conversion is not allowed.

## II. PARAMAGNETIC SCATTERING FROM Fe.

We illustrate in Fig. 2 our most recent results on Fe obtained by Wicksted et al.<sup>6</sup> These data clearly demonstrate the power of using polarization analysis. The basic principle of this technique was established by Moon, Riste, and Koehler<sup>8</sup> in 1969. Recently, Ziebeck and Brown and their collaborators<sup>9</sup> have put this technique to practical use. The reason for this delay of more than ten years is simply a matter of intensity. In 1969, it was estimated that the polarization analysis technique results in the loss of intensity by at least a factor of one hundred. Since then, considerable progress has been made in the development of polarizers, such as Heusler, <sup>57</sup>Fe and multilayer polarizers. In Fig. 2 our current set up utilizes Heusler crystals as monochromators and analyzers; this results in an intensity which is a factor of thirty weaker when compared with our best unpolarized set up which utilizes larger, focusing pyrolytic graphite monochromators and analyzers.

These profiles for paramagnetic scattering from Fe are considerably better than our earlier reports on Ni and Fe. This has been achieved through step by step improvements of all aspects of the polarized beam set up. The basic idea of this technique is extremely simple; the difference between the two cross sections obtained with the magnetic field at the sample  $H \parallel Q$  and  $H \perp Q$ , and with the flipper on, consists of magnetic scattering only. This completely eliminates the uncertainty of the background subtraction which is by no means trivial when the magnetic scattering is weak at high energy transfers as in Fig. 2(b). Notice the counting time depends rather strongly on the energy transfer because of the reactor spectrum. Thus the "ON" data which utilizes a horizontal magnetic field (HF) in Fig. 2(b) may be put into a definitive cross

section only after combining with the vertical magnetic field (VF) data, as shown in Fig. 2(c). Another interesting feature in Fig. 2(b) is how clearly the phonon cross section in the OFF data is separated out from the magnetic cross section.

These results, as well as similar data on Ni, can be interpreted in terms of a simple double Lorentzian scattering function

$$S(q, \omega) \propto \frac{1}{\kappa_1^2 + q^2} \cdot \frac{\Gamma}{\Gamma^2 + \omega^2} \cdot \frac{\omega/kT}{1 - e^{-\omega/kT}} \quad (1)$$

for energies  $\omega$  up to 50 meV and reduced wavevectors  $q$  up to  $0.5\text{\AA}^{-1}$ .  $\kappa_1$  is the inverse correlation length and  $\Gamma = Af(\kappa_1/q)q^{2.5}$ , where  $f(\kappa_1/q)$  is a dynamical scaling function, and the last term is the detailed balance factor, which of course should be included if  $\omega > kT$ . The model calculations by Uemura et al.<sup>8</sup> for Ni, using equation (1) and values for  $\Gamma$  and  $\kappa_1$  extrapolated from earlier critical scattering studies explained successfully the overall features of the constant E-scan ridges, although these calculations were performed in a simplified manner. The constant E ridges, previously identified as spin waves, are nothing but special energy slices of this paramagnetic scattering function.

There were, however, disagreements between the measured and calculated constant E ridge profiles. For example, the observed ridge positions are shifted to the higher  $q$  side of the broken line by about 40%. More recently, Lynn<sup>11</sup> emphasized that the measured ridge widths are significantly smaller than the predicted width. These difficulties are completely removed by the most

recent model calculations by Böni et al.<sup>12</sup> The only modification needed for Eq. (1) was to modify a pure Lorentzian  $\Gamma/(\Gamma^2 + \omega^2)$  to a slightly higher power at high  $\omega$ .

The results on Ni are quite similar to those of Fe. The smaller magnetic moment and the larger stiffness constant for Ni make the measurements more difficult. No propagating spin waves are observed up to 60 meV energy transfer.

### III. OTHER 3d FERROMAGNETS

We are now undertaking systematic studies of several other cubic ferromagnets utilizing the improved polarization analysis technique; these include EuO (insulator), Pd<sub>2</sub>MnSn (localized), Fe<sub>3</sub>Pt (invar), and MnSi (itinerant). These studies will be reported shortly. One feature which became convincingly clear is the common constant E-ridges above T<sub>c</sub>. In particular, the study of Pd<sub>2</sub>MnSn<sup>13</sup> permits us to cover the entire range of (Q,ω) because of the relatively low energy scale of this system. Again, the constant E ridges resemble spin waves below T<sub>c</sub> although constant Q profiles are smoothly diffusive up to the zone boundary. This is in marked contrast to the case of EuO, in which well defined magnons were observed<sup>14</sup> near the zone boundary between T<sub>c</sub> and 1.5T<sub>c</sub>. At present, it is not certain whether this different behavior is due to a long range interaction in Pd<sub>2</sub>MnSn or due to an intrinsic metallic nature of the magnetism.

One remarkable result of paramagnetic correlations in Pd<sub>2</sub>MnSn is the behavior of the line width  $\Gamma$  at large  $\zeta$  values, where a deviation from  $q^2$  behavior is expected. As shown in Fig. 3.,  $\Gamma(\zeta)$  shows an extremely simple behavior at 210°K (T<sub>c</sub> = 193K); namely  $\Gamma(\zeta)$  resembles the spin wave energy E(ζ) at low temperature.

$$\Gamma(\zeta) = \Lambda_1^* (1 - \cos 2\pi\zeta) \quad (2)$$

This equation is of course an approximation but it offers a very convenient way to parameterize the scattering function. We are now investigating the high temperature limit of paramagnetic scattering from Pd<sub>2</sub>MnSn.

#### IV. DISCUSSIONS

We have just demonstrated that all of the cubic ferromagnets we have investigated exhibit simple paramagnetic response above T<sub>c</sub> despite a wide range of characteristic parameters listed in Table I. Most of these parameters have been known from previous critical scattering work. We must introduce only one secondary parameter  $\alpha$  defined as<sup>1,2</sup>

$$S_Q(\omega) \propto \left( \frac{\Gamma}{\Gamma^2 + \omega^2} \right)^{1 + \alpha(\omega - \Gamma)/\Gamma} \quad (3)$$

This is a convenient way to convert a pure Lorentzian to a higher power at large  $\omega$ . As demonstrated for Fe, all characteristics of constant E ridges can be explained.<sup>6,12</sup> Notice that this introduction of  $\alpha$  affects only the higher  $\omega$  tails of the constant Q scans, though it has a rather dramatic effect on the constant E ridges.

In conclusion, we have demonstrated that the minor modifications in the tail of the paramagnetic scattering function, which are consistent with existing theories, resolve the disagreement with all available data; i.e. constant Q and constant E scans in Ni and Fe. We do not understand, however, why  $\alpha$  at T<sub>c</sub> selects such a value so that the constant E ridges resemble the spin wave dispersion curve below T<sub>c</sub>. Moreover,  $\alpha$  depends on temperature in such a way

that the expected rapid shift of the peak position immediately above  $T_c$  is compensated. The shift would be induced by the rapid change in  $\Gamma$  near  $T_c$  because of dynamical scaling. Probably, there is a simple basic underlying physics which keeps the ridge position fixed in the paramagnetic state. It is instructive to recall that model calculations of  $S(q, \omega)$  from very different starting points happen to resemble our contour maps. Better models may be found which describe the scattering more completely than the convenient double Lorentzian and may give further insight into the underlying physics.

Since constant E-scans have been widely used for many years when the stiffness constant is high, we ask the following question:<sup>12</sup> under which conditions are we not allowed to use the  $\Delta q \rightarrow \Delta E$  conversion? In Fig. 4(a) and Fig. 4(c) we have plotted two identical dispersion curves and indicated three different constant E-scans, which yield the same  $\Delta q$  widths for the same energy transfer. The same scans differ only in the sense that the peak intensities fall off faster with increasing energy in (c) than in (a). Case (a) results in propagating spin waves similar to what is sketched in (b) and the conversion  $\Delta q \rightarrow \Delta E$  is allowed; case (c) results in a diffusive mode (d) and the conversion  $\Delta q \rightarrow \Delta E$  is meaningless.

We would like to acknowledge many stimulating discussions with our collaborators P. Böni, Y. Endoh, Y. Ishikawa, C. Majkrzak, O. Steinsvoll, Y. J. Uemura, and J. P. Wicksted. Work at Brookhaven supported by The Division of Materials Sciences U. S. Department of Energy under contract DE-AC02-76CH00016. A part of this work was carried out under the program of the U.S.-Japan Collaboration on Neutron Scattering.

Table I. Cubic Ferromagnet

Parameters with \* refer to reduced unit  $\zeta$  in the (111) direction, except for Fe.

	Ni	Fe	Pd <sub>2</sub> MnSn	EuO
$T_c$ (°K)	631	1021	190	69
$D$ (0.8 $T_c$ )	350	175	70	7.4
$A$ (meV·Å <sup>2.5</sup> )	330	140	60	3.5
$A^*(\zeta)$	5600	2400	230	23
$\kappa_0^*(\zeta)$	0.20	0.34	0.22	0.30
$A_0$ (Å)	3.5	2.9	6.4	5.2
$d^*(nn)$	3.1	3.1	1.7	2.1

$$E = Dq^2, \Gamma = Aq^{2.5}, \kappa_1 = \kappa_0 \left( \frac{T-T_c}{T_c} \right)^{0.7}$$

References

1. Previous review was given by G. Shirane, O. Steinsvoll, Y. J. Uemura and J. Wicksted, J. Appl. Phys. 55 (1984) 1887.
2. H. A. Mook, J. W. Lynn and R. M. Nicklow, Phys. Rev. Lett. 30, (1973) 556.
3. J. W. Lynn and H. A. Mook, Phys. Rev. B 23, (1981) 198.
4. J. W. Lynn, Phys. Rev. B 11, (1975) 2624 and B 28 (1983) 6550.
5. O. Steinsvoll, C. F. Majkrzak, G. Shirane, and J. Wicksted, Phys. Rev. Lett. 51, (1983) 300 and Phys. Rev. B, to be published.
6. J. Wicksted, G. Shirane and O. Steinsvoll, Phys. Rev. B 29, (1984) 488 and J. Wicksted, P. Böni and G. Shirane, Phys. Rev. B, to be published.
7. P. J. Brown, H. Capellmann, J. Déportes, D. Givord and K. R. A. Ziebeck, J. Magn. Magn. Mat. 30, (1982) 243.
8. R. M. Moon, T. Riste and W. C. Koehler, Phys. Rev. 181 (1969) 920.
9. K. R. A. Ziebeck and P. J. Brown, J. Phys. F. Metal Phys. 10, (1980) 2015. P. J. Brown, H. Capellman, J. Deportes, D. Givrod and K. R. A. Ziebeck, J. Magn. Magn. Mat. 30, (1982) 243.
10. Y. J. Uemura, G. Shirane, J. Wicksted and O. Steinsvoll, Phys. Rev. Lett. 51 (1983) 2322.
11. J. W. Lynn, Phys. Rev. Lett. 52 (1984) 775.
12. P. Böni, G. Shirane, and J. Wicksted, to be published.
13. G. Shirane, Y. J. Uemura, J. Wicksted, Y. Erdoh, and Y. Ishikawa, Phys. Rev. B (submitted).
14. H. A. Mook, Phys. Rev. Lett. 46 (1981) 508.

FIGURE CAPTIONS

- Fig. 1. Constant E ridges for Ni. Solid and broken lines are the Oak Ridge results<sup>3,4</sup> which are in good agreement with our results, open and cross marks. After Steinsvoll et al.<sup>5</sup>
- Fig. 2. Magnetic cross sections of Fe below and above  $T_c$ . The experimental setup is shown in (d); Heusler polarizer and analyzer are combined with horizontal (HF) and vertical (VF) magnetic fields at the sample. The flipper F is placed after the sample for fixed  $E_F$ . After Wicksted et al.<sup>6</sup>
- Fig. 3. Line width  $\Gamma$  for the entire zone of (111) direction in  $Pd_2MnSn$ . After Shirane et al.<sup>13</sup>
- Fig. 4. Intensity profiles with identical positions and widths in constant E-scans (heavy horizontal lines) (a) and (c), but different peak intensities must be interpreted as spin waves (b) or energy slices of the paramagnetic scattering (d), respectively. After Böni et al.<sup>12</sup>

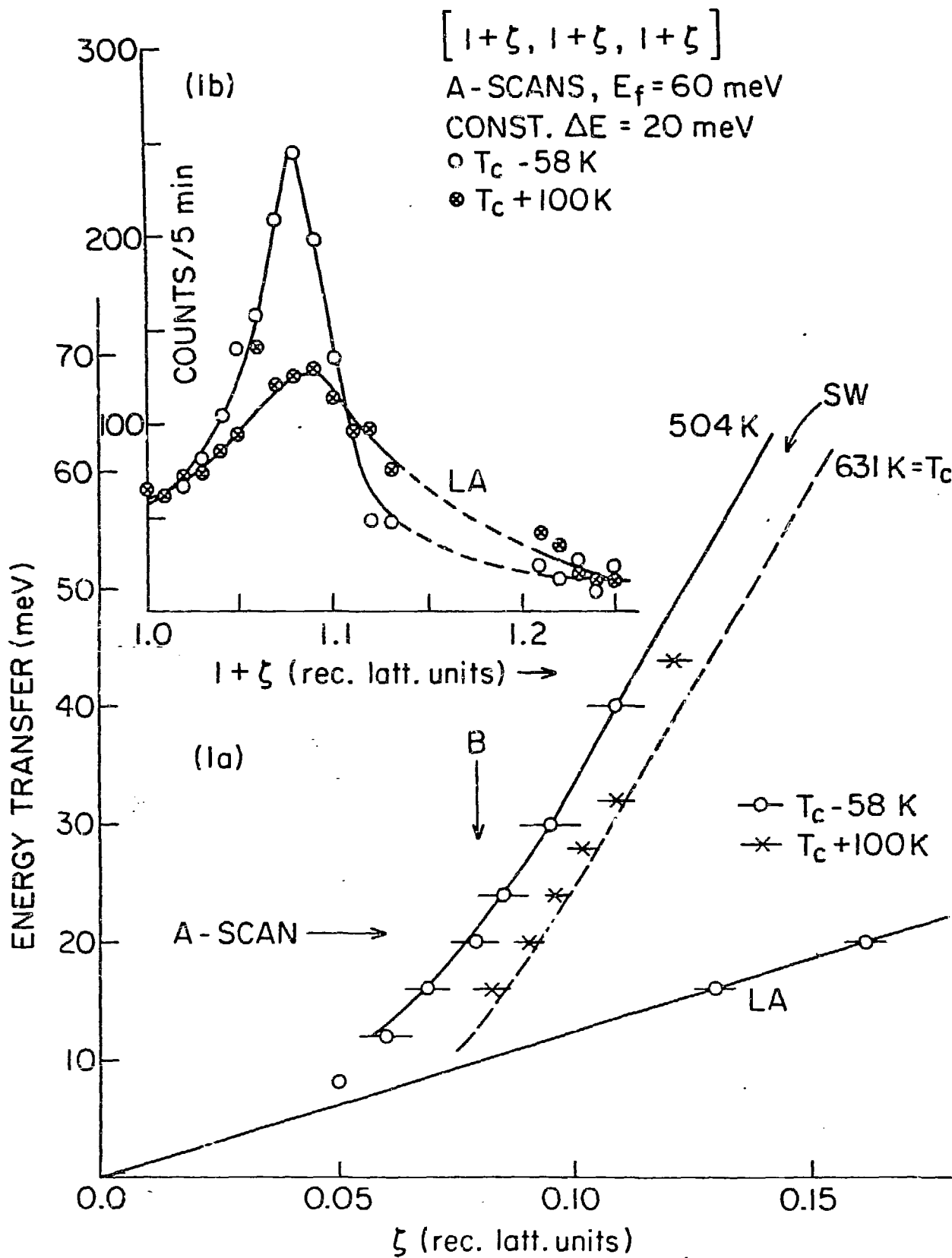


FIGURE 1

30.5 E<sub>F</sub> COLL: 40'-80'-80'-80'

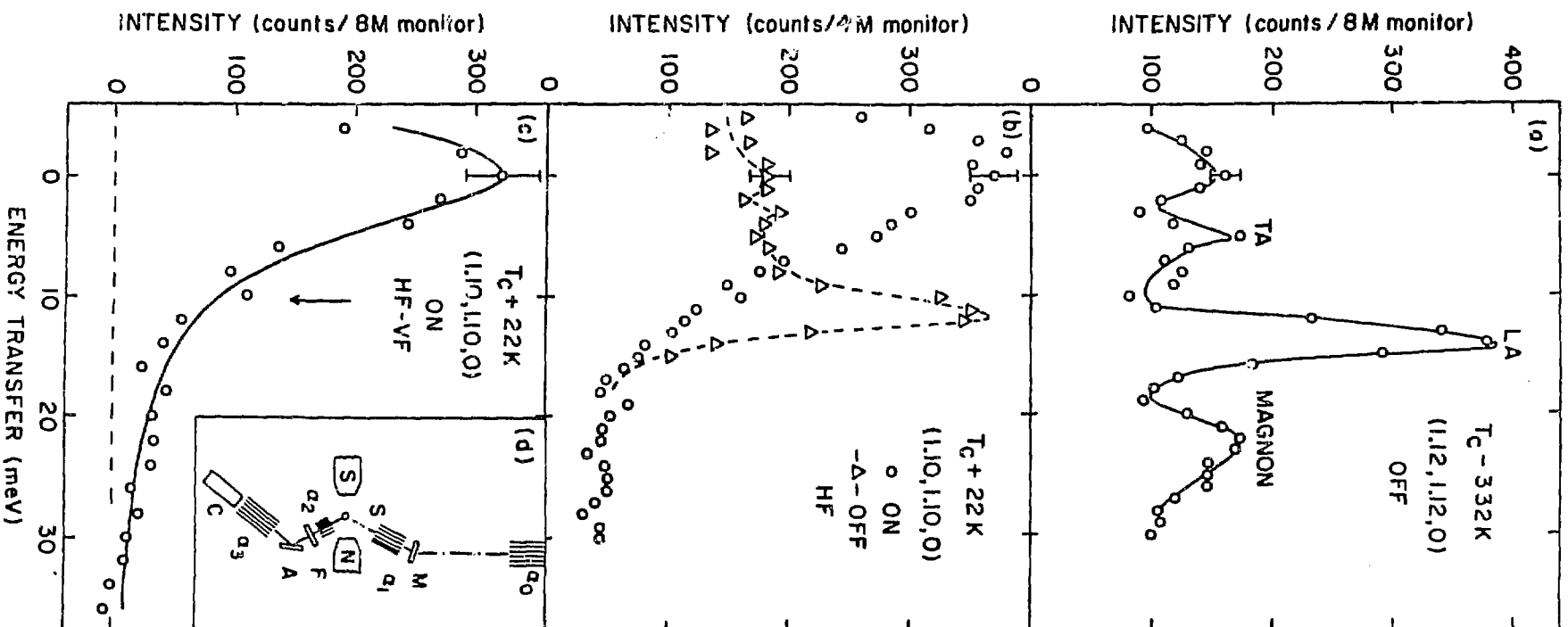


FIGURE 2

Pd<sub>2</sub>Mn Sn | T = 210°K

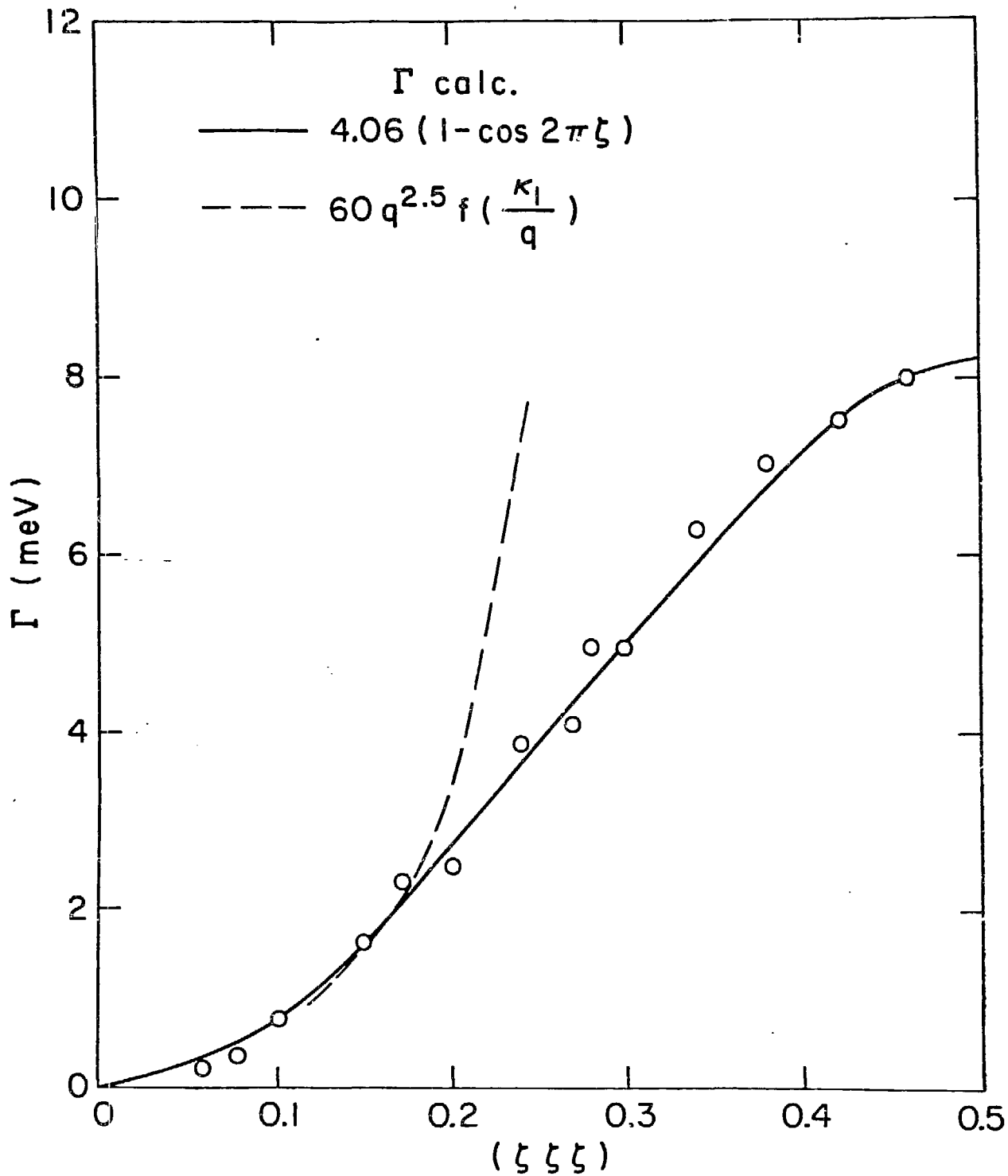


FIGURE 3

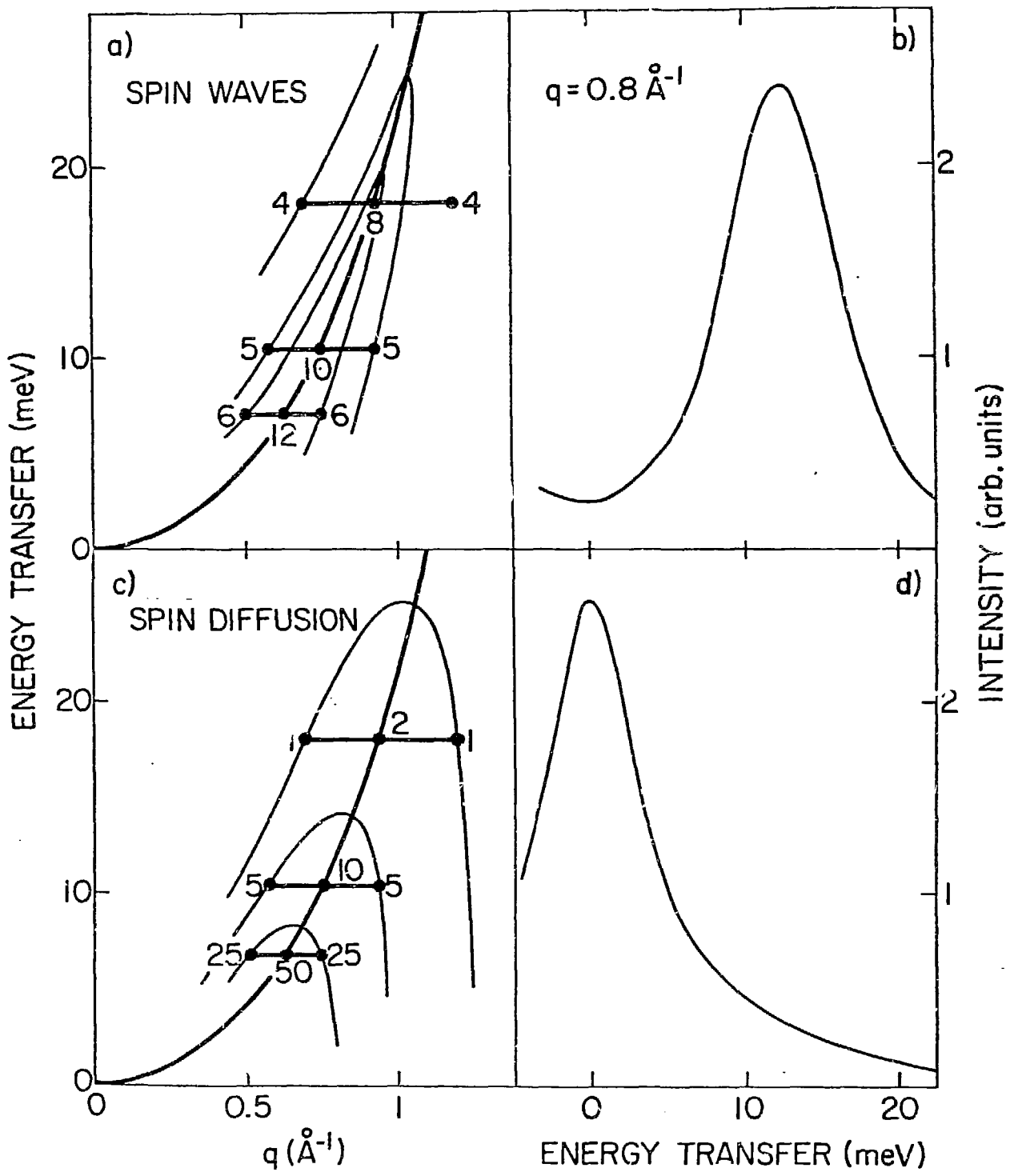


FIGURE 4